CURRENT-DENSITY DISTRIBUTION IN THE BEAM OF AN ARC PROTON SOURCE

V. N. Getmanov

UDC 621.384

The current-density distribution in the beam of an arc proton source is an important factor that determines the design and operation of the ion-optical system of a high-voltage accelerator. This distribution is studied for a pulsed arc source of hydrogen plasma with grid formation of the beam, whose design and operating conditions are discussed in [1-3].

1. Experimental Setup. The measurements were carried out on the setup shown in Fig. 1. Through the anode aperture 2 arc source 1 ejects a hydrogen plasma 4 onto grid-cathode diode 5, 6, which forms the initial proton beam. The diameter of the anode aperture is 2 mm and the aperture of the grids is circular with a diameter of 40 mm. An arc discharge is produced by pulses with length up to 100 μsec and repetition frequency 0.2 Hz, and the diode voltage U of up to 15 kV is kept constant. Coil 13, mounted on the arc-discharge chamber, moves along with it and generates a constant field with an induction that can be regulated from 0 to 0.64 mT. Grid diodes of two configurations, a Pierce diode similar to that described in [1, 3] and a planar diode, are used to form the beam. The electrode-holder of the cathode grid of the Pierce diode has a conical lug with a height of 14 mm and a slope of 64° to the angle of the beam. The current in the beam is measured by the signals I_h and I_g in the circuits of the high-voltage power supply and its anode grid. The formed H_+ proton beam enters transport tube 7, where its space charge is compensated by secondary electrons. The tube has an inside diameter of 42 mm and a length of 125 mm. The beam characteristics at the exit of the transport tube are measured by a multiwire x–y profilometer 8, 9, augmented with antidynatron rings 10 [4], as well as a small Faraday cup 11. The system is assembled inside a composite cylindrical magnetic shield 12 of mark-20 steel with inside diameter 100 mm, wall thickness 10 mm, and overall length 420 mm. The arrangement of the elements of the system is shown relative to the z axis, with origin at the position of the cathode grid of the diode. A vacuum of 0.2 mPa is produced in the system by two NORD-100 magnetic-discharge pumps.

2. Plasma-Density Distribution in the Jet. The Maxwell velocity distribution of the plasma protons ejected from the arc chamber through the anode aperture of radius r_0 should result in a Gaussian density distribution of the current j along the jet radius r, after expansion of the jet to a radius $R \gg r_0$, if the plasma spreads freely and the condition $E_0 \gg T$ is satisfied, where E_0 is the energy of the longitudinal motion of protons in the jet and T is the temperature of those protons, taken at the arc-chamber exit [1]. The current I_0 in the beam formed by a diode with a circular aperture of radius R_0 then is proportional to

$$i = 1 - \exp\left(-bR_0^2/l_0^2\right) \tag{1}$$

($b = E_0/T$, ℓ_0 is the base of the spread of the jet from the region where it formed to the cathode grid of the diode).

Figure 2 and Table 1 show the measured values of I_0 as a function of the distance ℓ from the anode aperture of the arc chamber to the cathode grid of the diode, which varied from 77 to 114 mm. In Table 1 the notation is as follows: j denotes the number of the measurement and σ is the relative error of the I_0 measurement. Since the tangent to the curve $f(\ell) = 1/\sqrt{i(\ell)}$, drawn at the point ℓ_* intersects the ℓ axis at the point $a = \ell_* - f(\ell_*)/(\partial f/\partial \ell)|_{\ell=\ell_*}$ on condition that $\ell - \ell_0 = \Delta\ell \ll \ell_*$, we obtain from (1) the equation

$$\Delta l/l = (E_1 - d_1)/(3E_1 - 2d(1 + d_1)), \tag{2}$$

where $E_1 = \exp(d) - 1$, $d = bR_0^2/\ell^2$, $d_1 = d(1 - a/\ell)$, and $\ell = \ell_*$. The straight line in Fig. 2 is drawn by the method of least squares from six points $f(\ell)$, which correspond to the largest values of ℓ at $89 \le \ell \le 114$ mm and intersects the ℓ axis at the point $a = -7 \pm 2.5$ mm.

Novosibirsk. Translated from Zhurnal Prikladnoi Mekhaniki i Tekhnicheskoi Fiziki, No. 1, pp. 3-8, January-February, 1991. Original article submitted April 21, 1987; revision submitted August 4, 1989.

0021-8944/91/3201-0001$12.50

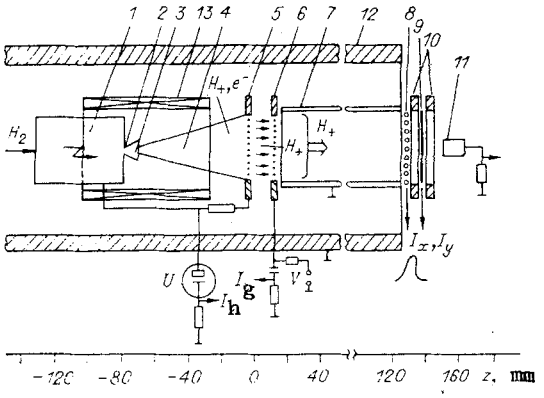

Fig. 1

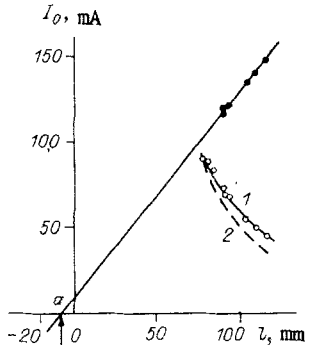

Fig. 2

TABLE 1

j	l, mm	I_0, mA	i_{exp}	σ	i_{calc}	j	l, mm	I_0, mA	i_{exp}	σ	i_{calc}
1	77	90,5	1,0	0,02	1,0	6	92	68	0,751	0,015	0,744
2	79	88,5	0,978	0,02	0,961	7	103	54,7	0,604	0,012	0,606
3	83	84	0,928	0,03	0,887	8	109	50,2	0,555	0,011	0,545
4	89	73,5	0,812	0,016	0,788	9	114	45,5	0,503	0,01	0,500
5	91	69	0,762	0,015	0,758						

Using this value of a, we can establish a relation between Δl and b from (2), where $l_* = 1/6 \sum_{j=4}^{9} l_j = 100$ mm, according to the data of Table 1. The use of (1) and (2) together makes it possible to organize a fitting procedure in which b is the largest parameter, Δl is determined from (2), and their combination is chosen by the criterion of maximum agreement between (1) and the experimental data on $I_0(l)$. The results of this procedure are given in Table 1 [i_{calc} was obtained from (1)] and are illustrated in Fig. 3. Goodness-of-fit test χ^2, in accordance with the ±2% error in the I_0 measurements, was calculated according to [5]. The minimum $\chi^2 = 3.4$ (the number of degrees of freedom was 8) was obtained at b = 8.5 and Δl = 14 mm and corresponds to a confidence level $P_1 = 0.85$ (Fig. 3, line 3), which is evidence of good agreement between the model of free spread of the plasma, reflected in (1), and the experiment. Lines 4 and 5 correspond to $P_1 = 0.8$ and 0.7.

Curve 1 in Fig. 2, drawn according to the points i_{calc}, is a good approximation of the experimental points $i_{exp}(l)$, which is the relative value of the current $I_0(l)$. Curve 2 corresponds to the model of collisionless uniform expansion of the plasma [8, p. 4], where $I_0 \sim l^{-2}$ [at $(R_0/l)^2 \ll 1$] but does not accord with the experimental data. The interval of allowable values of b and Δl at $P > 0.8$ has the form b = 7-9 and Δl = (10-16) mm, while at $P > 0.7$ it has the form b = 6.7-9.5 and Δl = (9-17.5) mm. This evidently means that the center of the region of nucleation of the plasma jet (see Fig. 1, curve 3) lies at $\Delta l = 14_{-4}^{+2}$ mm and the length of the region is $s_0 \approx 1$ cm. This very region (according to [6], where $\Delta l = 11_{-2}^{+3}$ mm, $s_0 < 15$ mm) is sensitive to weak magnetic fields with induction H > 1 G.

The radial plasma-density distribution on the cathode grid can be calculated in accordance with the model of free plasma expansion:

$$j(r) \sim \exp\left(-br^2/l_0^2\right). \tag{3}$$

The flux density at the edge of the grid aperture, i.e., at $r = R_0 = 20$ mm, is its relative maximum j_M = 42.5 and 71% at the axis when l = 77 mm and 114 mm, respectively. The figures were substantially lower, 91% and 96.5%, in the case of collisionless expansion, when $j \sim 1/(r^2 + l^2)$ [8]. In the case of free expansion the mean flux density $\langle j \rangle$, as follows from (3), is related to j_M by

$$\langle j \rangle = j_M [1 - \exp(-d_0)]/d_0 \quad (d_0 = bR_0^2/l_0^2). \tag{4}$$

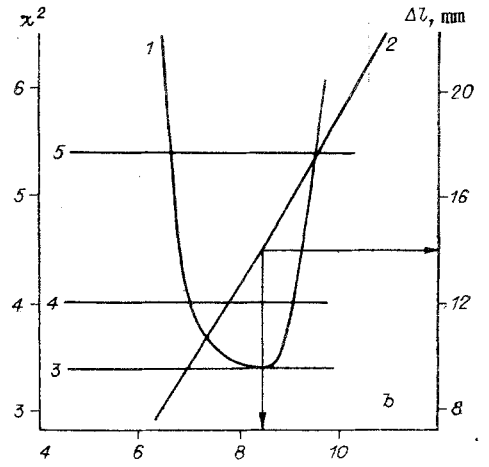

Fig. 3

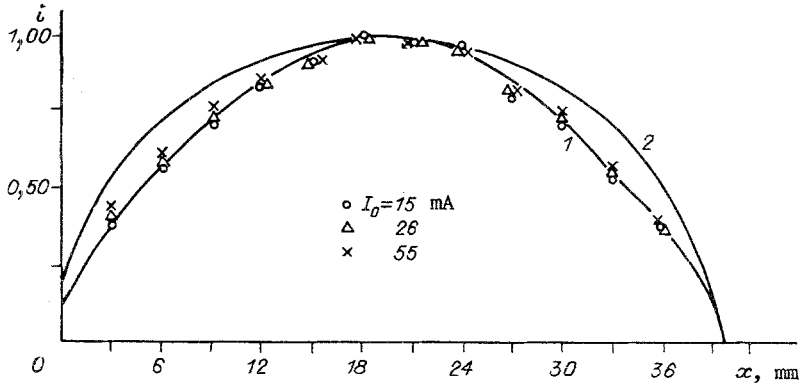

Fig. 4

It can be used to check the depth of plasma-density modulation at the cathode. This is done as follows: As the arc-discharge current increases smoothly we determine the time when the plasma enters the intergrid space, where the current density j_M on the diode axis exceeds j_0 (mA/cm²) = $1.72 \cdot U^{3/2}$ (kV)/L^2 (cm), following from the three-halves power law [7]. Such an experiment was carried out with a Pierce diode, in which the grid-plane separation L = 2.55 cm at U = 12.2 kV, which corresponds to j_0 = 11.3 mA/cm². The diameter of the grid filaments is 2ρ = 50 μm and the spacing pitch is s = 550 μm. The time when the plasma enters the intergrid space was determined from the abrupt expansion of the profile, accompanied by a change in its shape and the appearance of current-pulse oscillations. The measured current in the beam is I_0 = 91 ± 2.8 mA and the proton current in the diode, with allowance for the geometric transparency of the anode grid, is I_d = 100 ± 2 mA. From (4), bearing in mind that $j_M = j_0$, we find that the current in the diode should be equal to 95_{-4}^{+10} mA, which is in good agreement with the measured value of I_d and thus verifies (3).

3. Flux Profile. The Gaussian plasma-density distribution of the jet (3) at the cathode grid of the diode should lead to a Gaussian current-density distribution in the primary-beam cross section, which can be maintained during beam transport as well if the anode grid potential of the diode V = −100 V (see Fig. 1) is used to block the transport of secondary electrons and balance the proton space charge. Figure 4 shows the flux profiles measured by sensor 8, whose wires are oriented perpendicular to the filaments of the diode grids. A profile is characterized by 12 signals from information wires, which are made of 30-μm diameter gold-plated tungsten and arranged along the x axis on glass-textolite frames with a spacing of 3 cm. (The flux profile measured in the direction transverse to the wires of the diode grids by sensor 9, has the same shape and is 1-2 mm wider, because beam protons are scattered on inhomogeneities of the electric field near the grid wires.) The beam was formed with a planar diode, with the planes of its grids separated by a distance L = 14.2 mm (s = 225 μm, 2ρ = 50 μm). The profiles for three states of the beam with a current of 15, 26, and 55 mA were obtained at U = 10 kV, ℓ = 79 mm and other conditions fixed and is

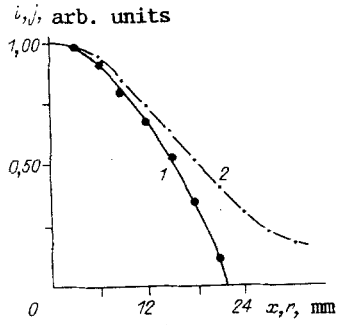

Fig. 5

virtually independent of the current, which is explained by the low current density in the beam. The signals from the wires of the sensor represent the integrals of the current along straight lines intersecting the beam cross section at different points; the distribution of the signals on the wires, therefore, should have the form

$$i(x) \sim \exp(-kx^2)\,\Phi\left(\sqrt{2k(R^2 - x^2)}\right), \tag{5}$$

where x is the minimum distance from the beam axis to the given wire; $k = b\ell_0^2$; R is the flux radius; and $\Phi(x) = 1/\sqrt{2\pi}\int_0^x \exp(-t^2/2)\,dt$.

A similar calculation within the framework of the model of collisionless expansion of a plasma [8] gives the condition

$$i(x) \sim \operatorname{arctg}\sqrt{(R^2 - x^2)/(l^2 - x^2)}. \tag{6}$$

In Fig. 4 curve 1 was drawn in accordance with (5) at b = 8.5, ℓ_0 = 65, and R = R_0 = 20 mm and approximates the experimental data well. Curve 2 was plotted according to (6) and is not in accord with experiment. This verifies the model of free plasma spreading and the efficacy of the system used to form and transport the proton flux.

The current-density distribution j(r) in the beam remains Gaussian at V = 0 as well (Fig. 5), but its slope increases. Curve 1 of Fig. 5 approximates the profile i(x) at b = 10. Curve 2, which was obtained from (3), gives the dependence j(r). At the same time, with rising V the current of the primary beam increases, indicating that the angle at which the plasma jet flies off decreases. These effects arise when the region of jet formation is acted upon by an electric field generated by electrons arriving from the transport tube at V ≥ 0. At high positive biases (V ~ 100 V), when the electron flux from the tube and the strength of the electric field scattering the proton beam in the tube increase considerably, the nature of the current-density distribution changes substantially. The drop in the current density in the central part of the transported beam, limited by the radius R ≈ 7.5 mm, speeds up while on the periphery of the beam, by contrast, it slows down considerably. The Gaussian approximation gives a good description of only the central part of the flux at R < 7.5 mm and then gives substantially underestimated values of the density, expecially as the bias V increases.

Dimov and Roslyakov [9] approximated the radial current-density distribution by using the function $j(r) \sim 1/(\ell^2 + r^2)^2$, which differs slightly from that used in [8] since in our case $(r/\ell)^2 \ll 1$. The explanation for the satisfactory result of such an approximation in [9] is apparently that the proton source operated under different conditions, in which a plasma jet with particle energy $E_0 \gg T$ is not formed and the plasma expands freely into the surrounding space.

Using the results of [3], where E_0 = 40 eV in a similar design, we obtain $T = E_0/b \approx (4.7_{-0.5}^{+1.2})$ eV, which is in accord with the data of [3, 8], where T = 4-5 eV. The values E_0/T = 7-9 and $\Delta\ell/r_0$ = 10-16 are higher than the values E_0/T = 4-6 and $\Delta\ell/r_0$ = 2-3 predicted by the simple scheme of ambipolar diffusion [10, p. 258]. This overestimation can be caused by preliminary acceleration of protons of the plasma jet to an energy of 10-12 eV in the region of the anode aperture of the arc chamber in accordance with the distribution of the

space potential (see [11]) and the distinctive design features of the anode attachment of the arc chamber, whose exit aperture is shielded by an 8-mm conical lug, as shown in Fig. 1. As a result of these effects the values of the parameters E_0/T and $\Delta\ell/r_0$ can increase by 2-3 and 8 units, respectively.

As mentioned by Getmanov and Savchenko [6], the shape of the plasma-density distribution in the jet does not change under the effect of a weak magnetic field while the density of the jet and the current of the beam formed from it increase; in the given case the current increases from 55 to 87 mA at H = 0.6 mT. This means that such action does not increase the emittance of the proton component of the jet.

The luminosity of the proton beam formed by the source can be determined by using the measured values of the proton emission temperature T_1 in the direction along the filaments of the grids, with allowance for the fact that under optimal diode operation, when the plasma boundary lies in the plane of the cathode grid, proton scattering on the inhomogeneities of the field of that grid is insignificant in comparison with scattering near the anode grid [1, 12]. During free spreading of the arc chamber to the grid diode the plasma jet expands by an order of magnitude in diameter and cools, hence $T_1 \gtrsim 40$ meV [3]. For beam protons scattered by the anode grid, the angular spread $\alpha = (s - 2\rho)/4L = 3.1$ mrad and corresponds to the energy spread $T_2 = qU\alpha^2 = 0.08$ eV. Hence, using the expression [1, 13] for the reduced emittance $\varepsilon = 2.1\cdot10^{-4}R_0\ (\text{cm})\cdot\sqrt{T\ (\text{eV})}$, we obtain $\varepsilon_1 \gtrsim 0.026\pi$ cm·mrad, $\varepsilon_2 \approx 0.035\pi$ cm·mrad, which at a beam current of 0.1 A corresponds to its luminosity $B = 2I_0/\varepsilon_1\varepsilon_2 \lesssim 45$ A/(cm²·mrad²).

The characteristics of the beam and the scheme of its formation have been used in the development of a high-voltage proton accelerator [14, 15].

LITERATURE CITED

1. V. I. Batkin, V. N. Getmanov, and O. Ya. Savchenko, "Increasing the luminosity of an arc proton source," Prib. Tekh. Éksp., No. 1 (1984).
2. V. I. Batkin, V. N. Getmanov, I. M. Ikryanov, and O. Ya. Savchenko, "Proton source with a regulated current for an electrostatic accelerator," Vopr. At. Nauki Tekh. Ser. Tekh. Fiz. Éksp., No. 1/22, Kharkov (1985).
3. V. I. Batkin, V. N. Getmanov, O. Ya. Savchenko, and R. A. Khusainov, "Diagnostics of a plasma jet by grid electrodes," Zh. Prikl. Mekh. Tekh. Fiz., No. 6 (1982).
4. V. N. Getmanov and V. I. Batkin, "Automated system for diagnostics of the beam of a proton source," Vopr. At. Nauki Tekh. Ser. Tekh. Fiz. Éksp., No. 2/4, Kharkov (1979).
5. L. N. Bol'shev and V. N. Smirnov, Tables of Mathematical Statistics [in Russian], Nauka, Moscow (1983).
6. V. N. Getmanov and O. Ya. Savchenko, "Effect of a weak magnetic field on the value of the current of an arc proton source," Zh. Prikl. Mekh. Tekh. Fiz., No. 3 (1987).
7. S. I. Molokovskii and A. D. Sushkov, Intense Electron and Ion Beams [in Russian], Énergiya, Moscow (1972).
8. V. I. Davydenko, G. I. Dimov, and G. V. Roslyakov, "Obtaining precision high-intensity ion and atomic beams," Preprint No. 83-18 [in Russian], Akad. Nauk SSSR. Sib. Otd., Inst. Yad. Fiz., Novosibirsk (1983).
9. G. I. Dimov and G. V. Roslyakov, "Development of atomic injectors for plasma heating and diagnostics," Institute of Nuclear Physics, Siberian Branch of the Academy of Sciences of the USSR, Vopr. At. Nauki Tekh. Ser. Termoyad. Sint., No. 3(16) (1984).
10. M. D. Gabovich, Physics and Technique of Plasma Ion Sources [in Russian], Atomizdat, Moscow (1972).
11. G. I. Dimov, Yu. G. Kononeko, O. Ya. Savchenko, and V. G. Shamovskii, "Experiments on obtaining intense hydrogen ion beams," Zh. Tekh. Fiz., 38 (1968).
12. G. I. Dimov and G. V. Roslyakov, "Pulsed charge-transfer source of negative hydrogen ions," Prib. Tekh. Éksp., No. 1 (1974).
13. V. A. Teplyakov and V. I. Derbilov, "Radiation of an axisymmetric ion beam," Prib. Tekh. Éksp., No. 1 (1969).
14. V. N. Getmanov and O. Ya. Savchenko, "Inventor's Certificate No. 1,494,840 SSSR," Otkryt. Izobret., No. 21 (1990).
15. V. N. Getmanov and O. Ya. Savchenko, "Application of a grid-stabilized plasma emitter in a system for forming a high-energy proton beam," Vopr. At. Nauki Tekh. Ser. Yad.-Fiz. Issled., No. 5/5 (1989).